JTTEE5 9:394-398

Nanopowder Deposition by Supersonic Rectangular Jet Impingement

V. Shukla, G.S. Elliott, and B.H. Kear

(Submitted 8 October 1999; in revised form 10 April 2000)

With a view toward developing the next generation of coatings using nanopowders, a cold gas dynamic spray (CGDS) technique has been investigated. In this method, a powder feeder is used to inject nanopowder agglomerates into a supersonic rectangular jet, with a design Mach number of 3.2. The powder particles gain speeds of up to 700 m/s through momentum transfer from the jet and bond to the substrate surface due to kinetic energy dissipation. Coatings of copper and nano-WC/10% Co on steel and aluminum substrates (3 to 5 μm in thickness) have been produced. The benefit of this process is that the material does not undergo any chemical changes during coating formation. To improve the quality of the coatings produced, the flapping motions produced by supersonic jet impingement were studied. Powder particle velocities and the jet impingement flow field were quantified using particle image velocimetry (PIV).

Keywords cold gas dynamic spray, nanostructured coatings, particle image velocimetry, supersonic jet impingement

1. Introduction

Thermal spraying has been widely used to apply protective coatings to parts and to repair worn out large diameter shafts in turbines and pumps. Most thermal spray processes currently used, *i.e.*, high velocity oxy-fuel, detonation gun, plasma spray, and arc spray, rely on high temperatures to heat up and melt the coating constituents during processing. This is a disadvantage if the material being coated has properties that degrade at high temperature. In cold gas dynamic spray (CGDS), the coating powder is injected into a supersonic jet, created from a converging-diverging nozzle, which then impinges on the substrate to be coated. The powder particles gain speed by momentum transfer from the high speed jet and bond to the substrate upon impact. The particles need to attain a velocity greater than a critical velocity for a bond to form; below this, critical velocity particles either bounce off the substrate or cause wear of the substrate material. This critical velocity depends on the material being sprayed. It has been reported to be approximately 450 m/s for copper powder impinging on a copper substrate.[1] The bond formed is solely due to the dissipation of the kinetic energy of the particles at the substrate surface. The benefit of CGDS is that the material is not heated in the jet to the point where any significant chemical changes are experienced, and the grain structure of the coating remains of the same order as the feed powder. Another advantage is the low residual thermal stresses in the coating.[2]

2. Experimental

The CGDS system, designed and built in house, is located in the Gas Dynamics and Laser Diagnostic Research Laboratory at Rutgers University. Compressors, dryers, an electric heater (60 kW), and high-pressure storage tanks of 8 m^3 at 17.2 MPa (2500 psi) supply the gas needed to run the CGDS system. A spray booth with dust collector, spark arrestor, and 4.4 m^3/s (10,000 cfm) blower, setup as a turnkey system by Hard Face Alloys Inc. (Santa Fe Springs, CA), facilitates safe testing of thermal spray systems. The current CGDS system has a maximum temperature and pressure of 315 °C (600 °F) and 5.5 MPa (800 psi). The converging/diverging supersonic nozzle (with a design Mach number of 3.2) has a rectangular exit of 3.17×16.23 mm and a throat area of 3.17×3.17 mm, which is similar to the CGDS nozzle used at Sandia National Laboratories (Albuquerque, NM).[3] A schematic of the experimental system is shown in Fig. 1(a). The supersonic airflow, with entrained powder particles, impinges normally on the substrate surface. The air supply, which passes through a heater, is controlled with a manual needle valve. The heater raises the air stagnation temperature, defined as the hypothetical air temperature achieved if the air flow velocity is reduced to zero adiabatically, and is a measure of the internal energy of the gas. The raised stagnation temperature helps the powder attain a higher exit velocity than without a heater. Powder is injected into the converging section of the nozzle, using a high operating pressure powder feeder designed for use with nanopowder agglomerates. The powder feeder is vibrated to promote formation of a "fluidized bed" of particles with bypass air that is introduced tangentially into a cylindrical cavity. The swirling motion entrains the particles up through the feeder, and the differential pressure adjustment across the feeder controls the particle feed rate. After being introduced into the nozzle (slightly upstream of the throat), the powder is accelerated by the supersonic nozzle. The dwell time of the powder in the hot gas is very brief, as the air cools rapidly during expansion. The powder particles are deposited onto a substrate that is translated back and forth; allowing several passes for a uniform coating. The powder feeder, nozzle, and translating mechanism are shown in Fig. 1(b).

Particle image velocimetry (PIV) was used as a flow diagnostic technique[4] In this technique, the air flow is mixed with small tracer particles and imaged by a pulsed laser sheet at known time intervals. Two images of each particle are thus formed. After recording the images, particle displacement and

V. Shukla, G.S. Elliott, and **B.H. Kear,** Center for Nanomaterials Research, Rutgers University, Piscataway, NJ 08854-8065. Contact e-mail: vishukla@jove.rutgers.edu.

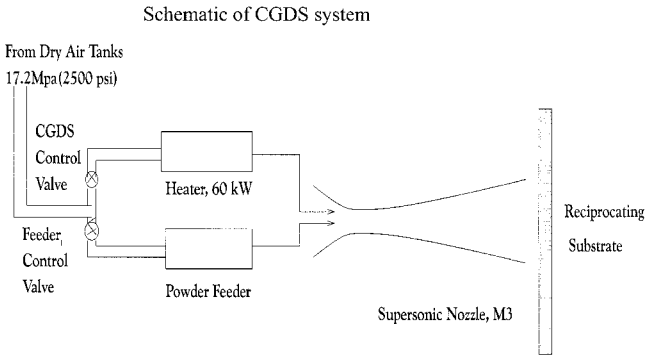

(a)

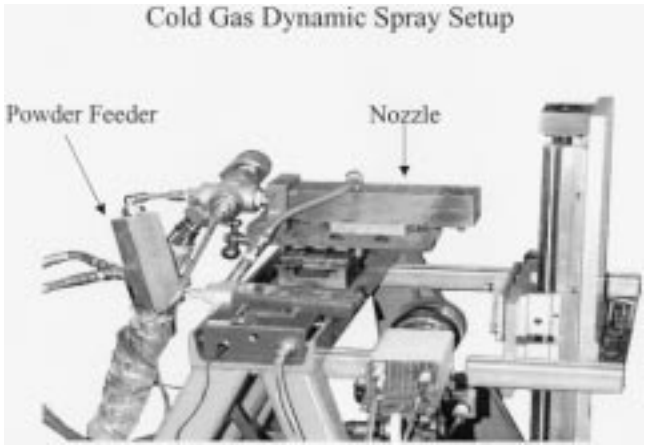

(b)

Fig. 1 (**a**) Schematic of the cold gas dynamic spray gun system and (**b**) photograph of the CGDS gun, powder feeder, and traverse mechanism.

velocity vectors for the imaged plane are determined using the two successive images and the known time elapsed between the images. Particle image velocimetry of the CGDS flow is performed using a 1000 × 1000 pixel Kodak Megaplus ES 1.0 camera fitted with a Nikor 200 mm lens. The laser sheet is formed from a dual cavity Nd:YAG laser (Model PIV200 from Spectra Physics, Mountain View, CA). The camera is operated in double pulse mode and is synchronized with the laser by using a delay generator (Model DG 535 from Stanford Research Systems, Sunnyvale, CA) and Imaging Technologies ICPCI board (Imaging Technologies, Bedford, MA) to acquire image pairs, with a time interval between pairs of 1.5 ms, at the rate of 10/s. The jet is seeded with zeolite particles (hollow spherical particles of less than 0.5 μm size) by injection into the nozzle throat using the particle feeder described above. Fog generated by a Roscoe fog generator (Roscoe Laboratories Inc., Stamford, CT) is used for seeding the outside flow. The image pairs are processed using cross-correlation data reduction, with 64 × 64 pixel interrogation windows and 75% overlap to determine the instantaneous velocity vector field at 16 pixel resolution, using software from Innovative Scientific Solutions Inc. (Dayton, OH). Average flow vector fields are generated by using 100 pairs of instantaneous vector fields.

3. Discussion of Results

In the past, a CGDS system has been used to produce coatings from micron-sized metal feed powders.[1,5,6,7] The present system was used to produce coatings from powders of 3 to 5 m copper, 1, 5, and 18 m size Al, and 40 m agglomerated nano-WC/10% Co on steel and aluminum substrates. A nozzle operating pressure of 3.1 to 3.4 MPa (450 to 500 psi) and stagnation temperature of 232 °C (450 °F) were used to produce these coatings. The particle velocity for the copper powder was estimated to be 700 to 750 m/s using PIV techniques, as described below. This exceeded the critical velocity of 450 m/s, which implied deposition efficiencies between 50 and 70%.[1]. The kinetic energy of the copper powder was such that particles deformed severely but did not melt. In the case of nano-WC/Co, the coatings were dense and experienced no decarburization. This is an advantage over conventional methods of depositing hard WC/Co coatings, which lose approximately 30% hardness due to decarburization at high process temperatures. So far, the coatings could only be built up to a thickness of 0.1 mm because of erosion of the deposited coating by the incoming powder. Some bounce-off of the powder was also observed

All coatings were analyzed by x-ray diffraction to check that the properties of the powders were unchanged due to the formation of oxides or decarburization. It can be observed from Fig. 2(a), for an aluminum coating, that the diffraction peaks from the powder (lower part of Fig. 2a) and coating line up, indicating that no new compounds were formed. Figure 2(b) is a 100× microscope image of the coating; the surface of the coating has pit marks formed by impact of the 44 to 74 m aluminum particles. These may have been formed by particles that did not have sufficient kinetic energies to bond with the existing coating. Porosity (27.2%) in a polished and etched aluminum coating is shown in Fig. 2(c). The porosity measurements were verified by using buoyancy measurements as specified in ANSI/ASTM-C20. These porosity measurements were performed only for aluminum coatings used made with the 45 to 74 m micron aluminum powder. A scanning electron microscope picture, (Fig. 2d) shows that coating formation is by plastic deformation of the powder particles.

Metal powder properties played an important role in the quality of coatings produced. This can be seen from Fig. 2(e) in which porosity of copper coatings, produced using the same flow parameters as the aluminum coating above, was only 4.3%. A possible explanation is the different critical velocities for copper and aluminum. Copper has a critical velocity of 450 m/s, while that for aluminum is 650 m/s[1] The measured particle velocities (approximately 700 m/s) were probably not fast enough to form dense aluminum coatings. The characteristic velocity for coating formation was noted to be dependent on the powder material and size. Preliminary results suggest that varying the nozzle-to-substrate stand-off distance between 20 and 50 mm does not change the porosity significantly. Qualitative results indicate that the particle size and nozzle operating conditions also affect the porosity of the coating.

Particle image velocimetry measurements were performed at stagnation pressure 3.1 MPa (450 psi) and stagnation temperature 15 to 20 °C (59 to 68 °F). In Fig. 3, the nozzle was located at x = 20, 40, and 62 mm and the flow is from right to left toward the substrate located at x = 0. The velocity vectors are drawn only in

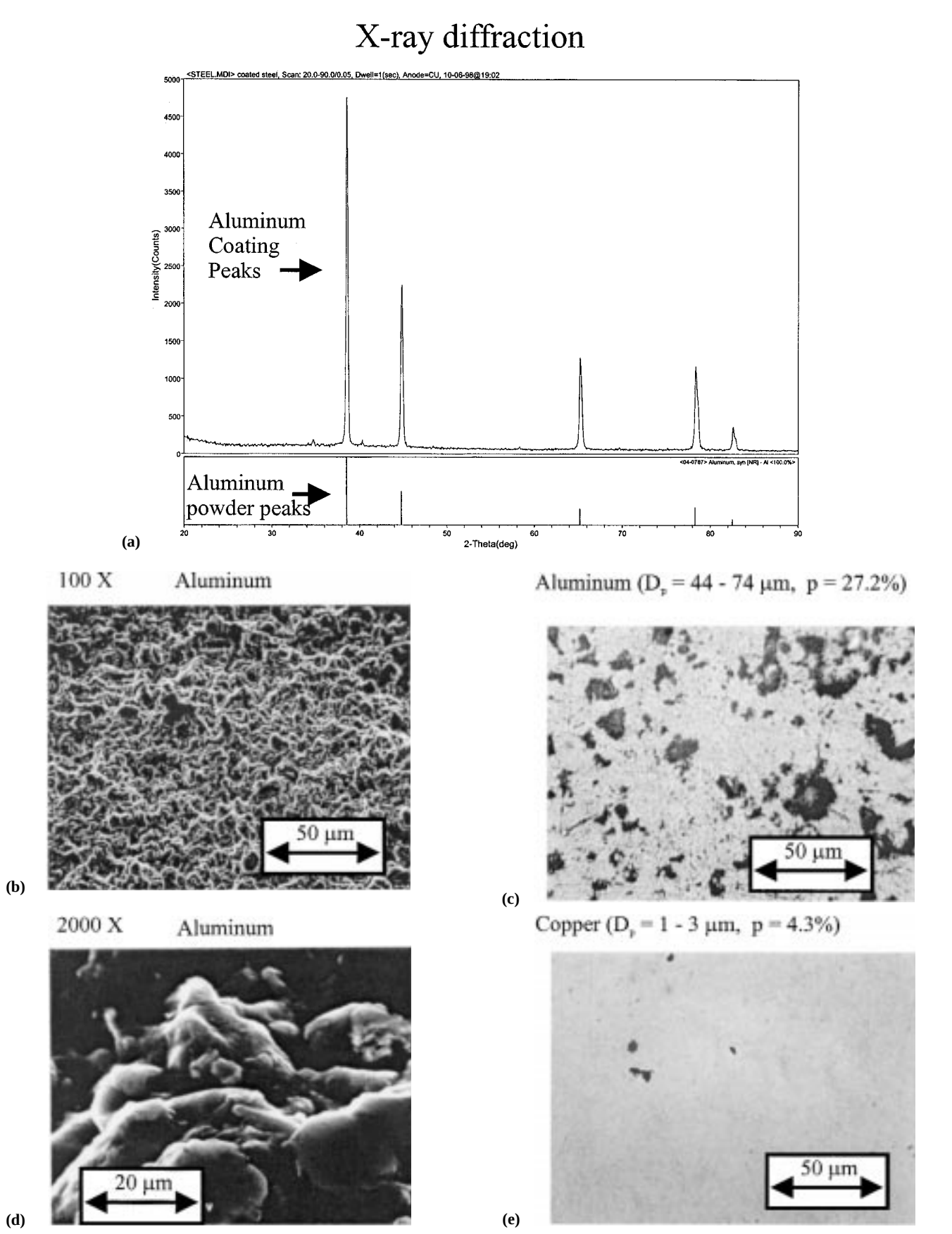

Fig. 2 (**a**) X-ray diffraction of an aluminum coating, (**b**) micrograph of Al coating, (**c**) porosity in etched Al coating, (**d**) 2000× scanning electron microscope picture of Al coating, and (**e**) porosity in copper coating.

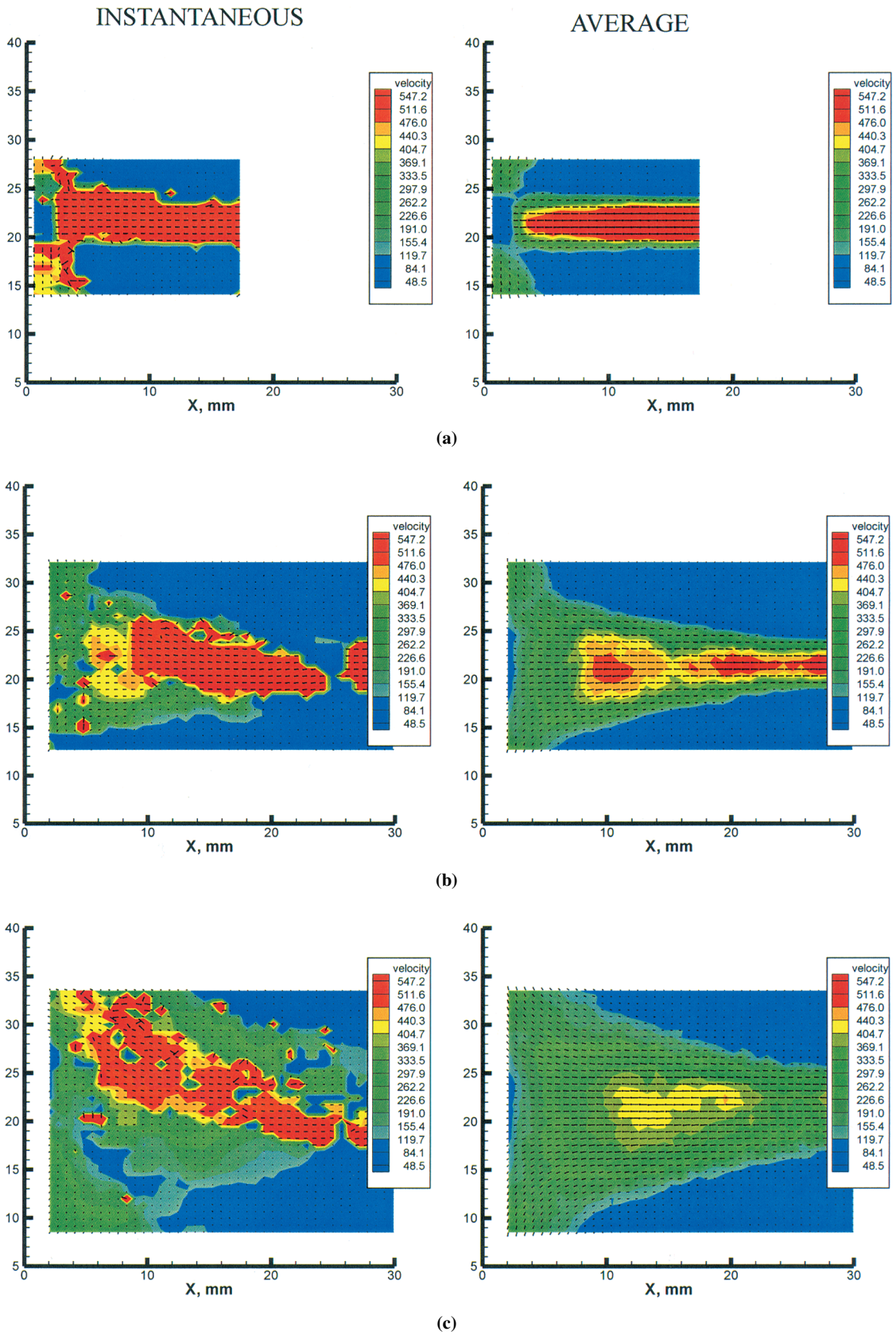

Fig. 3 Instantaneous and average vectors in close up of side view for stand-off distances of (**a**) 20 mm, (**b**) 40 mm, and (**c**) 62 mm.

the region surrounding the jet, and the velocity vector magnitude (m/s) is color contoured. The jet clearly can be seen in the side view vector images as the region of high velocity compared to the outer flow where the fluid velocities are low. The side view instantaneous vector plots (Fig. 3) show entrainment of ambient air into the jet, jet flapping (side to side motion), and deceleration of the jet as it approaches the substrate. A stagnation flow region, with the jet decelerating and changing direction, is formed in the region of impact of the jet with the substrate.

The upstream influence of the stagnation region increased in extent as the stand-off distance was increased, due to increased mixing associated with the flapping motion. The average flow fields show the jet size growth due to entrainment and flapping. The side view of the instantaneous vectors, Fig. 3(b) and (c), clearly shows the detail of the jet flapping. A stand-off plate shock, formed when the supersonic jet impinges on the substrate, can be seen in Fig. 3(a); the average flow field is located at approximately x = 2 mm. The vectors behind the shock suddenly reduce in magnitude. It is possible that the stand-off shock is not seen in Fig. 3(b) and (c), because not enough flow seed particles could be tracked in the planar sheet due to the highly three-dimensional nature of the flow field and the high vorticity near the stagnation region. As the stand-off distance is increased, the high velocity jet core disintegrates well before the impingement region due to flapping and entrainment of ambient air. Also apparent at larger stand-off distances are packets of high velocity fluid corresponding to the flapping modes. In the instantaneous velocity vector plots, regions of flow near the stagnation region, where the slow moving ambient air entrains into the jet core, are observed. The average jet approach velocity decreases significantly as the stand-off distance from the substrate is increased. The above PIV measurements show that the flow field near the coating formation region (jet impingement region) is extremely complex. In order to avoid the flapping motion in the jet, which sometimes peels the coating from the substrate, a short stand-off distance from the substrate is required.

Particle image velocimetry has also been used to measure the velocity of metal powder particles during the coating process. Using the operating pressure and temperature of 3.1 MPa (450 psi) and 232 °C (450 °F) and assuming isentropic conditions, the jet velocity was estimated as 820 m/s. In our experiment, copper powder was found to travel at speeds between 720 and 750 m/s and zeolite powder was found to travel between 760 and 780 m/s at the exit of the nozzle. The measured copper powder speed was higher than the critical velocity, and thus, we were able to produce dense coatings.

4. Conclusions

In CGDS, coatings are formed as a result of dissipation of kinetic energy of the particles upon impact with the substrate. Since the particles gain kinetic energy from the gas flow (inside the nozzle and in the supersonic jet prior to impact), the coating quality depends intimately on the flow conditions. As shown above, the flow near stagnation is complex. In order to form coatings, the particles need enough inertia to pass through the stand-off shock and stagnation flow mixing, and impinge on the substrate. If particles are small or too light, they will follow the flow and not form coatings. If the particles are too large, they do not gain enough kinetic energy to form a coating. Thus, only a small size range of particles can form coatings. Even when coatings form, the fluid dynamics can cause them to break off because of flapping motion. The present flow study justifies the choice of a short stand-off distance for CGDS operation, as the flapping motion is absent under these conditions. In the future, the flow results will be incorporated into models of coating formation, which may lead to a better understanding of the relation between coating formation and supersonic flow. Another observation worth mentioning is that when coatings of optimum quality are produced by CGDS, the jet noise has a distinct quality. Thus, it may be possible to optimize this coating process using an acoustic signature as a control parameter.

Acknowledgments

We acknowledge the support of the Office of Naval Research through Grant No. (N00014-97-1-0844) for the Advanced Coating Technology Development Program monitored by Dr. Lawrence Kabacoff. We also acknowledge the discussions on the CGDS process with Dr. R. Neiser, Sandia National Labs. Thanks are due to the staff at Rutgers University for help in running the nozzle and for analysis of coatings.

References

1. R.C. McCune, A.N. Papyrin, J.N. Hall, W.L. Riggs, and P.H. Zajchowski: in *Advances in Thermal Spray Science and Technology*, C.C. Berndt and S. Sampath, eds., ASM International, Materials Park, OH, 1995, pp. 1-6.
2. R.C. Dykhuizen and M.F. Smith: *J. Thermal Spray Technol.*, 1998, vol. 7 (2), pp. 205-12.
3. R. Neiser: Sandia National Laboratories, Albuquerque, NM, private communication, 1997.
4. V. Shukla and G.S. Elliott: *AIAA J.*, 1999, submitted for publication.
5. A.P. Alkimov, V.F. Kosarev, and A.N. Papyrin: *Dokl. Akad. Nauk USSR*, 1990, vol. 315, pp. 1062-65.
6. R.C. McCune, W.T. Donlon, E.L. Cartwright, A.N. Papyrin, E.F. Rybicki, and J.R. Shadley: in *Thermal Spray: Practical Solutions for Engineering Problems*, C.C. Brndt, ed., ASM International, Materials Park, OH, 1996, pp. 397-403.
7. R.B. Bhagat, M.F. Amateau, A.N. Papyrin, J.C. Conway, B. Stutzman, and B. Jones: in *Thermal Spray: A United Forum for Scientific and Technological Advances*, C. C. Berndt ed., ASM International, Materials Park, OH, 1997, pp. 361-67.